

## Original Research

# Expression of B-Cell Surface Antigens in Subpopulations of Exosomes Released From B-Cell Lymphoma Cells

Morten P. Oksvold, PhD<sup>1,2</sup>; Anette Kullmann, BS<sup>3</sup>; Lise Forfang, BS<sup>1,2</sup>; Bente Kierulf, BS<sup>3</sup>; Mu Li, PhD<sup>3</sup>; Andreas Brech, PhD<sup>2</sup>; Alexander V. Vlassov, PhD<sup>3</sup>; Erlend B. Smeland, MD, PhD<sup>1,2</sup>; Axl Neurauter, MSc<sup>3</sup>; and Ketil W. Pedersen, PhD<sup>3</sup>

<sup>1</sup>Department of Immunology, Institute for Cancer Research, Oslo University Hospital, Oslo, Norway;

<sup>2</sup>Centre for Cancer Biomedicine, University of Oslo, Oslo, Norway; and <sup>3</sup>Life Technologies AS, Oslo, Norway

### ABSTRACT

**Purpose:** Exosomes are small (30- to 100-nm) vesicles secreted by all cell types in culture and found in most body fluids. A mean of 1 mL of blood serum, derived from healthy donors, contains approximately 10<sup>12</sup> exosomes. Depending on the disease, the number of exosomes can fluctuate. Concentration of exosomes in the bloodstream and all other body fluids is extremely high. Several B-cell surface antigens (CD19, CD20, CD22, CD23, CD24, CD37, CD40, and HLA-DR) and the common leukocyte antigen CD45 are interesting in terms of immunotherapy of hematologic malignant neoplasms. The established standard for exosome isolation is ultracentrifugation. However, this method cannot discriminate between exosome subpopulations and other nanovesicles. The main purpose of this study was to characterize CD81<sup>+</sup> and CD63<sup>+</sup> subpopulations of exosomes in terms of these surface markers after release from various types of B-cell lymphoma cell lines using an easy and reliable method of immunomagnetic separation.

**Methods:** Western blotting, flow cytometry, and electron microscopy were used to compare the total preenriched extracellular vesicle (EV) pool to each fraction of vesicles after specific isolation, using magnetic beads conjugated with antibodies raised against the exosome markers CD63 and CD81.

**Findings:** Magnetic bead-based isolation is a convenient method to study and compare subpopulations of exosomes released from B-cell lymphoma cells. The data indicated that the specifically isolated vesicles differed from the total preenriched EV pool. CD19, CD20, CD24, CD37, and HLA-DR, but not CD22, CD23, CD40, and CD45, are expressed on exosomes from B-cell lymphoma cell lines with large heterogeneity among the different B-cell lymphoma cell lines. Interestingly, these B-cell lymphoma-derived EVs are able to rescue lymphoma cells from rituximab-induced complement-dependent cytotoxicity.

**Implications:** Distribution of exosomes that contain CD19, CD20, CD24, CD37, and HLA-DR may intercept immunotherapy directed against these antigens, which is important to be aware of for optimal treatment. The use of an immunomagnetic separation platform enables easy isolation and characterization of exosome subpopulations for further studies of the exosome biology to understand the potential for therapeutic and diagnostic use. (*Clin Ther.* 2014;36:847–862) © 2014 The Authors. Published by Elsevier HS Journals, Inc.

**Key words:** B-cell lymphoma, B-cell surface antigens, exosomes, flow cytometry, immunotherapy, magnetic beads.

Accepted for publication May 16, 2014.

<http://dx.doi.org/10.1016/j.clinthera.2014.05.010>  
0149-2918/\$ - see front matter

© 2014 The Authors. Published by Elsevier HS Journals, Inc. This is an open access article under the CC BY-NC-ND license (<http://creativecommons.org/licenses/by-nc-nd/3.0/>).



Scan the QR Code with your phone to obtain FREE ACCESS to the articles featured in the Clinical Therapeutics topical updates or text GS2C65 to 64842. To scan QR Codes your phone must have a QR Code reader installed.

## INTRODUCTION

The current understanding of the nature of exosomes is that they are small (30- to 100-nm) cargo-containing vesicles secreted by all cell types in culture. In addition, exosomes have been found in body fluids, such as blood, saliva, urine, and breast milk.<sup>1</sup> Exosomes have been found to be involved in a variety of different biological processes, such as antigen presentation,<sup>2</sup> apoptosis, angiogenesis, inflammation, and coagulation.<sup>3</sup> They can exchange proteins and lipids with target cells to initiate downstream signaling pathways and deliver specific nucleic acids.<sup>4-6</sup> Exosomes are formed by a process in which endosome membranes invaginate to form vesicles inside the endosomal compartment, producing multivesicular bodies (MVBs). They can contain nucleic acids in the form of microRNA and mRNA,<sup>4,7-9</sup> whereas less ribosomal RNA (rRNA) has been found.<sup>10</sup> The protein composition of exosomes reflects their endocytic origin in addition to their possible role in intercellular communication.<sup>11</sup> Exosomes contain proteins from the membrane and fusion machinery (GTPases, annexins, and flotillin), MVB formation machinery (Alix and TSG101), tetraspanins (CD9, CD63, CD81, and CD82), heat shock proteins (Hsp70 and Hsp90), and lipid-related proteins and phospholipases.<sup>12,13</sup> The exosomal expression of these proteins is cell type dependent.

Isolation of exosomes is generally performed by ultracentrifugation often in combination with sucrose density gradients or sucrose cushions to float the exosomes and thereby obtain high enrichment.<sup>14</sup> Other, less elaborate size-based isolation procedures have been performed with ultrafiltration protocols.<sup>15</sup> Precipitation-based protocols in combination with low-speed centrifugation or filtration have been reported to isolate all exosomes in the sample.<sup>16-18</sup> To obtain ultrapure exosome preparations or isolation of potential subpopulation of exosomes, an immunomagnetic isolation strategy can be applied by targeting exosomal markers.<sup>19,20</sup>

A large number of studies have reported that tumor-derived exosomes can enhance cancer progression and suppress immune responses. Interestingly, exosomes have also been reported to contain oncogenes derived from originating tumor host cells,<sup>21</sup> indicating the possible use of exosomes as samples for early detection of cancer markers. The procancer effect of exosomes derived from cancer host cells also affects the cancer treatment by causing treatment resistance. It is well known that B cells transformed with the Epstein-Barr virus contain large numbers of MVBs, which spontaneously fuse with the

plasma membrane and release numerous exosomes, containing molecules essential for the adaptive immune response.<sup>22</sup> Several components of the B-cell receptor complex have been detected in extracellular vesicles (EVs),<sup>23-25</sup> which are vesicles shed from the plasma membrane.<sup>26-29</sup> The role of exosomes in B-cell biology is potentially interesting for early diagnostic applications and in terms of their putative role in tumor immunotherapy. Development of more potent vaccines with exosomal targeting in some viral and parasitic diseases has been suggested as a possible approach.<sup>30</sup> Exosomal B-cell antigens might intercept immunotherapy. Aung et al<sup>31</sup> recently detected antigens that affect established immunotherapy treatment (eg, expression of CD20 on exosomes from B-cell lymphoma cells correlates negatively with rituximab [anti-CD20] treatment). The epitope-specific binding of anti-CD20 antibody was found to disturb the treatment with rituximab, reducing the available antibodies binding to the tumor cell in addition to complement consumption and inhibition of complement-dependent cytotoxicity of cancer cells.<sup>31</sup> Interestingly, increased cytolytic activity of rituximab against tumor cells was observed after removal of the exosomes. A similar scenario may also be possible for antibodies against other B-cell surface antigens (eg, CD19, CD22, CD23, CD37, CD40, and HLA-DR), which are currently in clinical trials.<sup>32-34</sup> This finding indicates that targeting the exosomes would be advantageous to increase the efficacy of therapeutic antibodies.

The aim of our study was to establish an easy and reliable method to characterize subpopulations of exosomes released from different cell lines that represent various types of B-cell lymphoma. We analyzed the expression of 9 different B-cell surface proteins (CD19, CD20, CD22, CD23, CD24, CD37, CD40, CD45, and HLA-DR), which are interesting in terms of immunotherapy for depletion of B cells and hematologic malignant neoplasms.<sup>32-39</sup> Using this method, we characterized differences in protein composition between exosomes derived from different sources and found heterogeneity in the exosomal expression of B-cell surface antigens among B-cell lymphoma cell lines. We found that EVs derived from lymphoma cells are able to intercept rituximab-induced complement-dependent cytotoxicity (CDC). In addition, CD19, CD20, CD24, CD37, and HLA-DR were detected in different exosome populations released from B-cell lymphoma cells, which can have an effect on immunotherapy.

## MATERIALS AND METHODS

### Reagents

For isolation of CD63<sup>+</sup> exosomes, magnetic beads coated with monoclonal anti-human CD63 were used (Exosome-Human CD63 Isolation/Detection; Life Technologies, Oslo, Norway). For isolation of CD81<sup>+</sup> exosomes, magnetic beads coated with monoclonal anti-human CD81 (Life Technologies) were applied. The primary antibodies for Western blotting analysis were as follows: mouse anti-CD81 (sc-7637), anti-CD9 (sc-59140), anti-CD45 (sc-1178), and anti-HLA-DR (sc-53319) and goat anti-CD19 (sc-8498) and anti-CD20 (sc-7733) (Santa Cruz Biotechnology, Santa Cruz, California). Mouse anti-human CD63 (antibody 59479) was obtained from Abcam (Cambridge, Massachusetts). The primary antibodies for flow cytometry were as follows: mouse anti-human CD9 phycoerythrin (PE) (555372), anti-human CD63 PE (556020), anti-human CD81 PE (555676), anti-human CD22 antigen-presenting cell (APC) (333145), anti-human CD23 PE (561774), anti-human CD24 PE (555428), and anti-human CD40 APC (555591) (all from BD Biosciences, San Jose, California). Anti-human CD19 Alexa-488 (MHCD1920), anti-human CD45 APC (MHCD4505), and anti-human irrelevant isotype-matched APC-labeled monoclonal antibodies (MG105) were purchased from Invitrogen (Carlsbad, California). Anti-human CD20 PE (R7013) was obtained from Dako (Carpinteria, California), and anti-human HLA-DR fluorescein isothiocyanate (FITC) was from eBioscience (San Diego, California). Mouse anti-human CD37 (HH1), originally developed in our laboratory,<sup>40</sup> was obtained from Diatex Monoclonals AS (Oslo, Norway) and Nordic Nanovector (Oslo, Norway) and coupled to Alexa-647. Horseradish peroxidase-coupled goat anti-rabbit IgG and rabbit anti-mouse IgG and anti-goat IgG were obtained from Dako. Horseradish peroxidase-coupled anti-mouse IgG Trueblot was purchased from eBioscience. Protein-A gold was obtained from CMC (Utrecht, Netherlands). All other reagents were from Sigma-Aldrich (St. Louis, Missouri) unless otherwise noted.

### Cell Culture

The B-cell lymphoma cell lines Ramos, SUDHL-4, SUDHL-6, and Ros-50 were maintained in RPMI 1640 (PAA, Pasching, Austria) supplemented with 10% fetal bovine serum (FBS; Lonza, Basel, Switzerland), penicillin, and streptomycin. The colon adenocarcinoma SW480

cell line was maintained in RPMI 1640 (Lonza), supplemented with 10% FBS (Gibco, Carlsbad, California), L-glutamine, and 0.01% sodium pyruvate. Cells were routinely tested for mycoplasma (Venor GeM; Minerva Biolabs, Berlin, Germany).

### Exosome Extraction From Cell Media

Before harvesting exosomes, the cell culture medium was replaced with fresh complete medium with FBS for 24 hours. Ramos, SUDHL-4, SUDHL-6, and Ros-50 cells ( $1 \times 10^8$ ) and SW480 cells ( $5 \times 10^7$ ) were cultured for each exosome sample preparation. After 24 hours, cells and debris were removed by centrifugation at 350g for 10 minutes and 2000g for 30 minutes. The Total Exosome Isolation Kit (Life Technologies) was added to the cell and debris-free cell medium (1:2 with exosome isolation reagent and cell medium, respectively). Cell medium and the exosome isolation reagent were mixed by brief vortexing and incubated at 4°C overnight before centrifugation at 4°C at 10,000g for 1 hour. The pellet that contained pre-enriched exosomes was resuspended in phosphate-buffered saline (PBS) (eg, 400 µL for 10 mL of cell media input). During all exosome sample preparations, negative controls were made from the corresponding complete medium with FBS. Before analysis of pre-enriched exosome samples, total protein level was measured using Bio-Rad protein assay (Bio-Rad Laboratories, Hercules, California) and Sunrise microplate absorbance reader (Tecan, Männedorf, Switzerland) and adjusted to equal total protein concentrations.

### Size of Exosomes

Analysis of pre-enriched exosomes was performed using the NanoSight LM10 instrument (Malvern Instruments Company, Nanosight, Malvern, United Kingdom), following the manufacturer's protocol. Precipitated exosomes from the culture media of  $50 \times 10^6$  SW480 cells were resuspended in 1 mL of PBS. Input was 5 µL, and measurement volume was 1 mL.

### Real-Time Quantitative Polymerase Chain Reaction

RNA isolation, reverse transcription, and real-time quantitative polymerase chain reaction analysis were performed as previously described.<sup>41</sup> The following primers were used for the experiment: Hs99999905\_m1 (GAPDH), Hs03023880\_g1 (ACTB), Hs99999901\_s1 (18S), has-let-7a, 000377 (Let7a), and has-miR-16, 000391 (miR16).

### Immunolabeling of EVs for Ultrastructural Analysis

Preenriched EVs (5  $\mu$ L) were placed on carbon-coated copper grids and incubated for 15 minutes at room temperature followed by blocking with 0.5% bovine serum albumin (BSA) in PBS for 10 minutes and embedded in methylcellulose. A standard immunogold labeling procedure<sup>42</sup> that targeted CD81 was performed. Then EVs were analyzed at the Unit of Cellular Electron Microscopy, Oslo University Hospital, on a JEOL JEM 1230 transmission electron microscope (Jeol Ltd, Tokyo, Japan). Images were recorded at 80 kV using a Morada camera and iTEM software (Olympus, Tokyo, Japan). Further image processing was performed with Adobe Photoshop software (Adobe Systems, San Jose, California).

### Preparations of Total Cell Samples for Western Immunoblotting Analysis

Cells were lysed and processed for SDS-PAGE as described previously.<sup>43</sup> SuperSignal West Dura or Femto (Thermo Scientific, Waltham, Massachusetts) was used for detection. Chemidoc MP (Bio-Rad Laboratories) or Hyperfilm (GE Healthcare, Buckinghamshire, England) were applied for imaging.

### Preparation of Preenriched Exosomes for Western Immunoblotting Analysis

The total preenriched exosome sample was diluted 1:1 in PBS, 5 $\times$  RIPA lysis buffer and proteinase inhibitor (F. Hoffmann-La Roche AG, Basel, Switzerland) was added, and the sample was incubated at 4°C for 15 minutes. The lysed exosomes sample was mixed 1:1 with 2 $\times$  Tris lysis buffer (pH 6.8) under reducing or nonreducing conditions. Samples were further processed for SDS-PAGE.

### Preparation of immunoisolated Exosomes for Western Immunoblotting Analysis

The total preenriched exosome sample was diluted 1:1 in PBS with 0.1% BSA. Magnetic beads coated with anti-human CD63 or anti-human CD81 (200  $\mu$ L of 2  $\times$  10<sup>6</sup> immunomagnetic beads) were prewashed, mixed with the exosome sample, and incubated overnight at 4°C while mixing. The beads were washed in PBS with 0.1% BSA and lysed in 25  $\mu$ L of RIPA buffer (150 mM sodium chloride, 1.0% NP-40, 0.5% sodium deoxycholate, 0.1% SDS, 50 mM Tris, pH 8.0) with proteinase inhibitors followed by 15-minute

incubation on ice. The lysate was mixed 1:1 with 2 $\times$  Tris lysis buffer under reducing or nonreducing conditions. Samples were further processed for SDS-PAGE.

### Preparation of Exosomes on Immunomagnetic Beads for Electron Microscopy

Immunomagnetic beads coated with anti-human CD81 (50  $\mu$ L) were mixed with total preenriched exosome sample (250  $\mu$ L) followed by overnight incubation at 4°C. The sample was centrifuged shortly on a table centrifuge to collect all material. Then PBS with 0.1% BSA (500  $\mu$ L) was added to the sample followed by mixing. The tube was then applied to a magnetic field and supernatant was removed.

### Electron Microscopy

For conventional Epon embedding and sectioning, exosomes isolated with immunomagnetic beads coated with anti-human CD81 were fixed in 1% glutaraldehyde in 200 mM cacodylate buffer (pH 7.4) for 1 hour, washed repeatedly in dH<sub>2</sub>O, and incubated in cacodylate buffer that contained 1.5% potassium ferricyanide and 1% osmium tetroxide for 1 hour. After 2 subsequent 30-minute incubations in 1% tannic acid and 1.5% magnesium uranyl acetate, the samples were dehydrated by using ethanol and embedded in Epon. Ultrathin sections were prepared and stained with lead citrate. Sections were analyzed on a Philips CM100 (Electron Microscopy Unit for Biological Sciences, University of Oslo).

### Flow Cytometry

Subpopulations of exosomes were isolated from total preenriched exosome samples using immunomagnetic beads coated with anti-human CD81. The beads (20  $\mu$ L) were washed before adding preenriched exosome sample (100  $\mu$ L) and PBS with 0.1% BSA (150  $\mu$ L). The beads were incubated overnight at 2°C to 8°C while mixing. After incubation, the beads were washed by using magnet separation and PBS with 0.1% BSA. After washing, beads were resuspended in 300  $\mu$ L of PBS with 0.1% BSA. A volume of 100  $\mu$ L was used for each flow staining and incubated for 45 to 60 minutes in a shaker (1050 rpm) at room temperature followed by washing and flow cytometric analysis using fluorescence-activated cell sorting (FACS) (BD FACS-Canto II, BD Biosciences and Cytobank Inc, Menlo Park, California).

## Viability Assay

SUDHL-6 cells ( $2 \times 10^5$  per well in a 96-well plate) cultured with complete RPMI 1640 with noninactivated human serum (20%) were incubated or not with precipitated EVs (10–20  $\mu\text{g}/\text{mL}$ ) derived from SUDHL-6 or SW480 cells and then rituximab was added (1  $\mu\text{g}/\text{mL}$ ). The cells were incubated for 1 hour and then incubated with 20  $\mu\text{L}$  of CellTiter 96 Aqueous One Solution reagent (Promega, Fitchburg, Wisconsin) for 1 hour. Absorbance at 490 nm was measured in a Sunrise 96-well plate reader (Tecan).

## RESULTS

### Analysis of Exosome Markers and B-Cell Surface Antigens in Cells

To characterize exosomes from different B-cell lymphoma cells, we first analyzed the expression of classic exosomal markers and B-cell surface antigens in cells by Western immunoblotting of total cell lysates and by flow cytometry at the single-cell level. CD9, CD63, and CD81, members of the tetraspanin family of proteins, are frequently located at the exosome surface.<sup>11,44–46</sup> Chiba et al<sup>47</sup> found that the tetraspanin protein family (CD9, CD63, and CD81) was a useful collection of markers of exosomes derived from colorectal cancer cell lines, including SW480. The SW480 cell line was therefore chosen as a positive control for exosomal markers. Furthermore, exosomes derived from SW480 were used as negative controls for the analysis of B-cell surface protein because of the lack of CD19 and CD20, surface molecules that are expressed in all B-lineage cells.<sup>48</sup>

CD63 and CD81 were detected in lysates from all cell lines. CD81 expression was low in SW480 compared with B-cell lymphoma cell lines, CD63 expression was low in SUDHL-6 cells and highest in SW480 cells, and CD9 was expressed only in SW480 cells (Figure 1A), as expected. Expression of the 4 different B-cell surface antigens (CD19, CD20, CD45, and HLA-DR) was detected in all B-cell lymphoma cell lines, except HLA-DR, which was absent or weakly expressed in Ramos cells (Figure 1A) in agreement with previous findings.<sup>32</sup> Different CD45 isoforms were detected, which has previously been described in B-cell lymphoma cells.<sup>49</sup> Furthermore, CD45 is heavily glycosylated, which can explain the observed smearing of CD45 (Figure 1A). As expected, expression of B-cell surface antigens was not detected in SW480 cells. Flow cytometry was applied to

characterize the expression of 5 additional B-cell surface antigens (CD22, CD23, CD24, CD37, and CD40) in the different B-cell lymphoma cell lines (Figure 1B). CD37 was highly expressed in all cell lines (Figure 1B), whereas expression of CD24 was detected in 2 of the cell lines (SUDHL-6 and Ros-50). CD22 was well expressed in all cell lines, CD40 was moderately expressed, and CD23 was weakly expressed.

### Analysis of Exosome Markers and B-Cell Surface Antigens in Preenriched Exosome Samples

Next, exosomes were preenriched by precipitation and centrifugation of cell culture supernatants harvested from cells in culture for 24 hours. The size distribution of the precipitated exosomes from SW480 cell culture media was analyzed using the NanoSight LM10 instrument, which had a size range (maximum, 102 nm) comparable to standard exosome preparations by ultracentrifugation (Figure 2A). Furthermore, to verify that precipitated exosomes were comparable in terms of RNA content, the precipitated exosomes originating from the SW480 cells were analyzed for mRNA, rRNA, and microRNA content. In agreement with earlier studies,<sup>4,8</sup> the precipitated exosomes contained full-length mRNA and rRNA (GAPDH and 18S) and microRNAs (ACTb, Let7a, and miR16), which are typical for exosomes (Figure 2B). To confirm the identity of these vesicles, the preenriched samples were subjected to immunolabeling followed by contrasting before ultrastructural analysis. Preenriched exosome samples were prepared from all 4 different B-cell lymphoma cell lines in addition to SW480 cells. In this approach, only antigens located on the surface of the exosomes are available for antibody binding, such as the tetraspanin protein CD81, commonly identified in exosomal preparations.<sup>50</sup> Ultrastructural analysis confirmed that the observed vesicles represented exosomes in terms of size and expression of CD81 (Figure 2C). These preenriched exosomes, which had a homogenous size distribution as previously reported,<sup>41</sup> were present in the culture media from all 5 different cell types analyzed.

Lysates of the preenriched exosome samples were then analyzed in more detail for expression of B-cell surface proteins and exosome markers by Western immunoblotting. Our complete RPMI media with FBS was analyzed for possible contents of exosomes. The

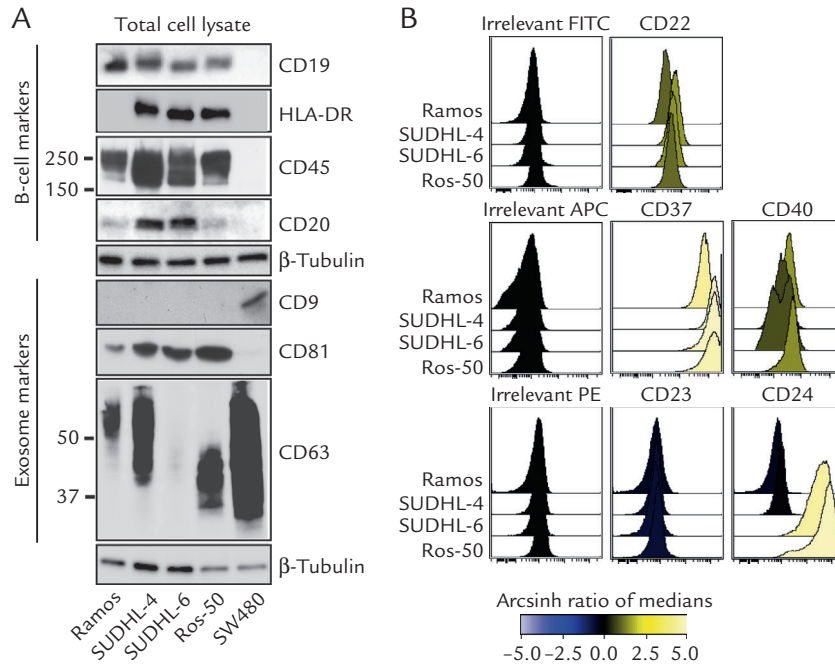
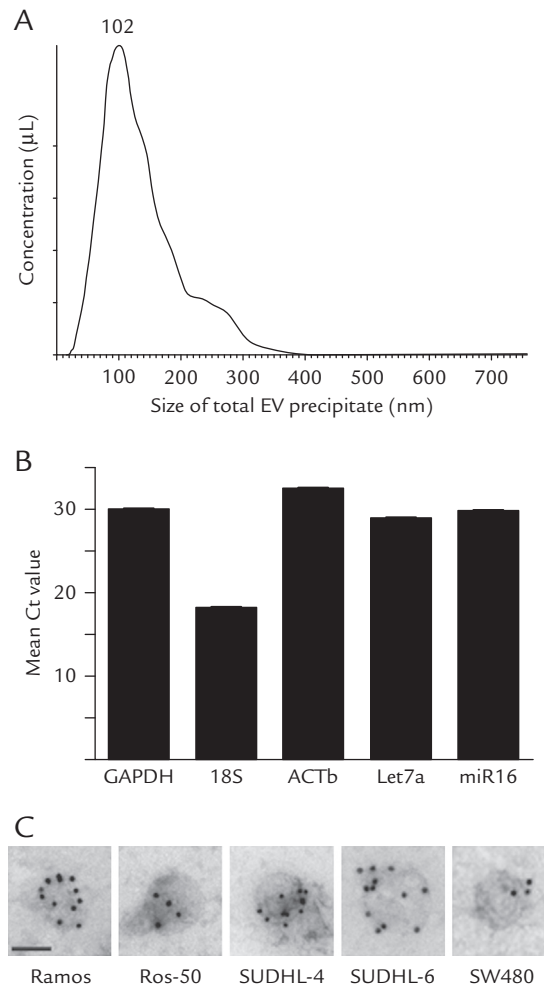


Figure 1. Expression of B-cell surface proteins and exosomal markers. (A) Total cell lysates from 4 different B-cell lymphoma cell lines (Ramos, SUDHL-4, SUDHL6, and Ros-50) and SW480 cells were lysed and processed for Western immunoblotting analysis. Expression of the B-cell surface proteins (CD19, CD20, CD45, and HLA-DR) and exosomal proteins (CD9, CD63, and CD81) were studied.  $\beta$ -Tubulin was applied as the loading control. One of 3 representative experiments is shown. (B) Cells were stained with a panel of antibodies against B-cell surface proteins (CD22, CD23, CD24, CD37, and CD40) or irrelevant control antibodies on ice for 30 minutes. Median fluorescence intensity (arcsinh ratio of medians) relative to irrelevant control is shown. Fluorescence-activated cell sorting (FACS) analysis was performed on singlet cells using BD FACSCanto II. One of 3 representative experiments is shown. APC = antigen-presenting cell; FITC = fluorescein isothiocyanate; PE = phycoerythrin.

exosome markers human CD81 and CD63 were not detected in precipitates from complete RPMI media with FBS, but precipitates from the same culture media incubated with cells for 24 hours contained CD81 and CD63 (Figure 3A). Total expression of CD81 and CD63 was also compared between the ultracentrifuged and precipitated exosomes, which had an expression comparable to these exosome markers (Figure 3B). The abundance of HLA-DR in preenriched exosome samples mirrored the expression of this protein in the parental cells, whereas the exosomal expression levels of CD19, CD20, and CD45 were more limited in preenriched exosomes compared with the more or less abundant expression in the host cells (Figure 3C; compare with Figure 1A).

CD19 was only detected in preenriched exosome samples from SUDHL-6 cells. CD45 was not detected in preenriched exosome samples from Ramos cells. CD20 was only detected in preenriched exosome samples from SUDHL-4 and SUDHL-6 cells (Figure 3C). The expression of the general exosome markers (CD63 and CD81) in preenriched exosome samples had a pattern similar to total cell samples, although the expression levels of CD81 was somewhat different (Figure 3A; compare with Figure 1A). Exosomes released from SUDHL-6 cells had strong staining for CD81 but low expression of CD63. In contrast, exosome samples from SW480 had high expression of CD63 and low expression of CD81. Precipitated exosomes were also analyzed for possible



**Figure 2.** Analysis of precipitated exosomes. (A) Precipitated extracellular vesicles (EVs) from SW480 culture media were analyzed by NanoSight LM10. The size distribution of total EV precipitate resuspended in phosphate-buffered saline is shown. (B) Precipitated exosomes released from SW480 cells were analyzed for the content of typical exosomal mRNA and ribosomal RNA (GAPDH and 18S) and microRNAs (ACTB, Let7a, and miR16) by real-time quantitative polymerase chain reaction. Mean (SD or SEM) threshold cycle (Ct) values for 3 independent experiments are shown ( $n = 3$ ). (C) Immunolabeling of exosomes derived from 4 different B-cell lymphoma cell lines (Ramos, SUDHL-4, SUDHL6, and Ros-50) and SW480 cells. Preenriched exosomes were transferred to copper grids and immunostained with mouse anti-human CD81 followed by rabbit anti-mouse antibody and colloidal gold coated with protein A (10 nm). Samples were stained with uranyl acetate. One of 3 representative experiments is shown. Scale bar = 100 nm.

contamination from intracellular nonexosomal proteins. The heat shock protein gp96 is constitutively expressed and located in the lumen of the endoplasmic reticulum, and the expression of this protein was analyzed in our precipitated exosomes derived from B-cell lymphoma

and SW480 cell lines. gp96 was not detected in any of the exosome samples but was highly expressed in cell lysates (Figure 3D), indicating that precipitated exosomes are not contaminated by unwanted intracellular proteins or endoplasmic reticulum fragments.

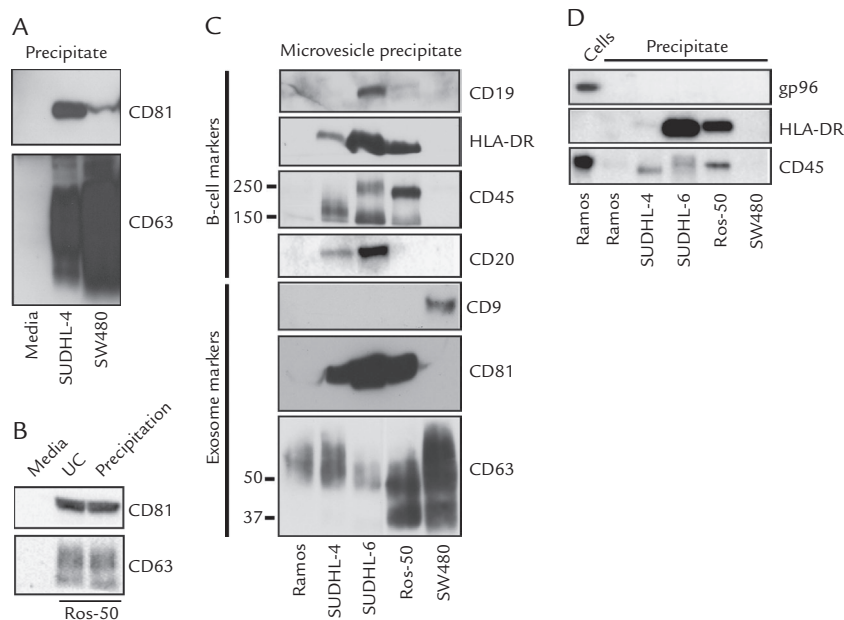


**Figure 3.** Expression of B-cell surface proteins and exosomal markers in preenriched exosomes. (A) Precipitates from complete RPMI media and media from SUDHL-4 and SW480 cells were lysed and processed for Western immunoblotting analysis. Expression of the exosomal proteins CD81 and CD63 were analyzed. One of 3 representative experiments is shown. (B) Exosomes from Ros-50 cells preenriched by ultracentrifugation (UC) or precipitation were analyzed by Western immunoblotting with antibodies against CD81 and CD63. Precipitates from complete RPMI media were used as the negative control. One of 3 representative experiments is shown. (C) Preenriched exosomes in media from 4 different B-cell lymphoma cell lines and SW480 cells were lysed and processed for Western immunoblotting analysis. Expression of the B-cell surface proteins (CD19, HLA-DR, CD45, and CD20) and exosomal proteins (CD9, CD63, and CD81) was analyzed. One of 3 representative experiments is shown. (D) Precipitates were also analyzed for possible contamination of an irrelevant endoplasmic reticulum protein (gp96). Total cell lysate (Ramos) and precipitates from the indicated cell lines were analyzed by Western immunoblotting against gp96 in addition to HLA-DR and CD45. One of 3 representative experiments is shown.

### Analysis of Exosome Subpopulations

The standard method for exosome sample preparation is ultracentrifugation. A challenge with this method is lack of specificity in terms of type of vesicles. Often, the vesicles obtained by this method have a heterogeneous size distribution, indicating that other vesicles are coenriched.<sup>51</sup> To increase the sensitivity, remove potential protein aggregates enriched together with EVs, and possibly isolate subpopulations of exosomes, we applied immunomagnetic separation to isolate exosomes that expressed CD63 and CD81 from cell culture media. Before a detailed Western immunoblotting and flow cytometric analysis

of exosomes isolated with immunomagnetic beads, we analyzed the magnetic bead-bound exosomes at the ultrastructural level. We also compared exosomes isolated by ultracentrifugation and precipitation after capture on anti-human CD81 antibody-coated beads. Ultrathin sections of anti-human CD81 beads preincubated with exosomes derived from SW480 cell cultures were made and subjected to electron microscopy to visualize the efficiency of exosome docking (Figure 4). The exosomes observed had a narrow size distribution (approximately 100 nm), similar to what has been previously reported.<sup>19,51</sup> Exosomes isolated by ultracentrifugation (Figure 4A) and precipitation



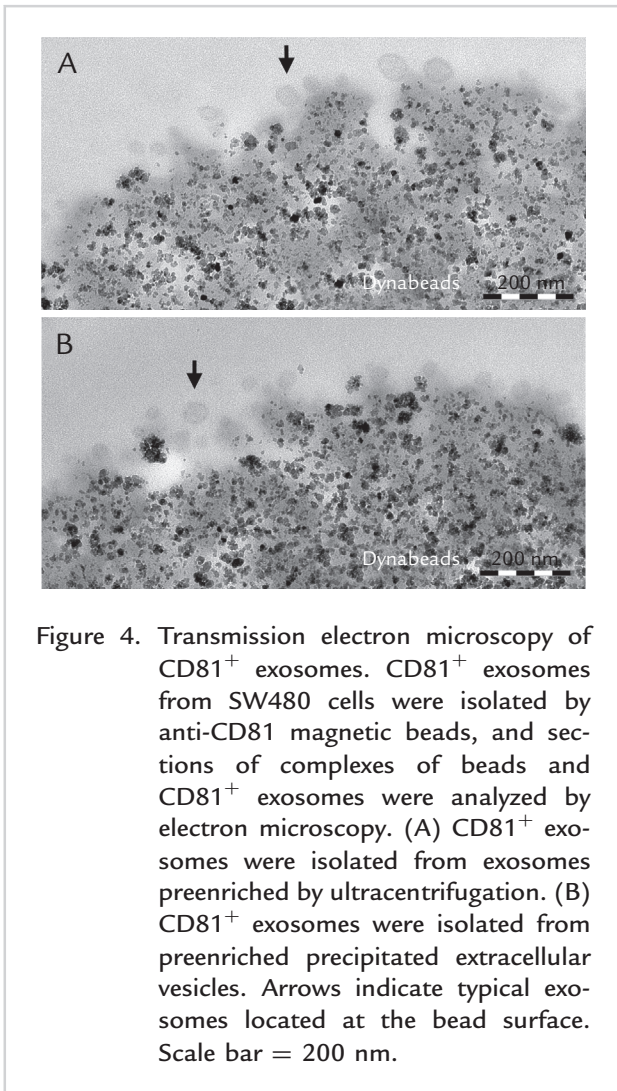


**Figure 4.** Transmission electron microscopy of CD81<sup>+</sup> exosomes. CD81<sup>+</sup> exosomes from SW480 cells were isolated by anti-CD81 magnetic beads, and sections of complexes of beads and CD81<sup>+</sup> exosomes were analyzed by electron microscopy. (A) CD81<sup>+</sup> exosomes were isolated from exosomes preenriched by ultracentrifugation. (B) CD81<sup>+</sup> exosomes were isolated from preenriched precipitated extracellular vesicles. Arrows indicate typical exosomes located at the bead surface. Scale bar = 200 nm.

(Figure 4B) were comparable in terms of size and morphologic features, although the exosomes preenriched by ultracentrifugation appeared somewhat more heterogeneous in terms of size. The exosomes appeared electron dense, spherical, and evenly distributed as single structures (no aggregates) at the surface of the magnetic beads. The density of exosomes was proportional to the number of exosomes present in the sample solution (data not shown).

Exosome capture on immunomagnetic beads allowed us to provide a docking surface for the exosomes required for downstream flow analysis and for enrichment of CD63<sup>+</sup> and CD81<sup>+</sup> human exosomes for Western immunoblotting analysis. A total of 9 B-cell surface proteins were analyzed for expression in

subpopulations of exosomes. The expression levels of the B-cell surface proteins CD19, CD20, CD45, and HLA-DR were low on exosomes compared with the preenriched exosome samples (Figures 5A, 5B, 5C, and 5D). Of interest, CD45 was not detected in exosome samples. For CD63<sup>+</sup> exosomes, HLA-DR was the only B-cell surface protein that was detected and mainly in media from Ros-50 cells (Figure 5A; quantification in Figure 5B). CD19, CD20, and HLA-DR were detected in CD81<sup>+</sup> exosomes from SUDHL-6 cells (Figure 5C; quantification in Figure 5D). In addition, HLA-DR was detected in CD81<sup>+</sup> exosomes from Ros-50 cells (Figure 5C). The low abundance of B-cell surface proteins was partly reflected by the expression of exosome markers. CD81 and CD63 were detected in all exosome samples but at highly variable relative expression levels. For the exosomes isolated with anti-human CD81 beads, high expression of CD81 was seen in SUDHL-6 and Ros-50 exosomes, whereas high expression of CD63 was only seen in Ros-50 exosomes (Figure 5A and 5C). The exosomes isolated with anti-human CD63 beads revealed a more uniform relative expression of CD81 versus CD63 for all lymphoma cell lines. However, of the 4 B-cell lymphoma cell lines, only Ros-50-derived exosomes had high CD63 expression levels. We also compared bead isolation of CD81<sup>+</sup> exosomes from ultracentrifuged and precipitated EVs and analyzed the samples for the expression of CD81 and CD63. The expression level of CD81 and CD63 was comparable between samples that were either ultracentrifuged or precipitated initially (Figure 5E).

#### Analysis of CD81<sup>+</sup> Exosomes by Flow cytometry

We proceeded with isolation and downstream flow cytometric analysis of CD81<sup>+</sup> exosomes. The exosome size precludes analysis by FACS alone given the limited resolution of the flow cytometer. Therefore, a solid support at a size detectable by flow cytometry is required. To obtain a strong flow signal, the concentration of magnetic beads was kept low. In this way, each magnetic bead was loaded with sufficient exosomes. The forward and side scatterplot revealed how the magnetic beads appear in flow cytometry and how the gating is performed (Figure 6A). The fluorescence histogram reveals the background median fluorescence intensity of the magnetic beads. Immunomagnetic isolation of exosomes and staining with isotypic antibody revealed a similar profile, indicating that background

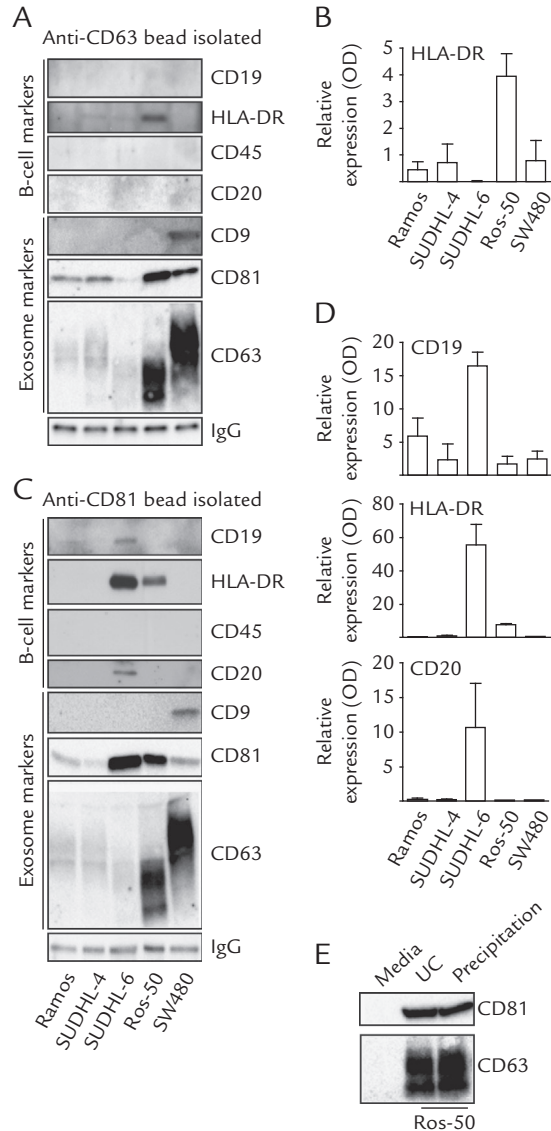
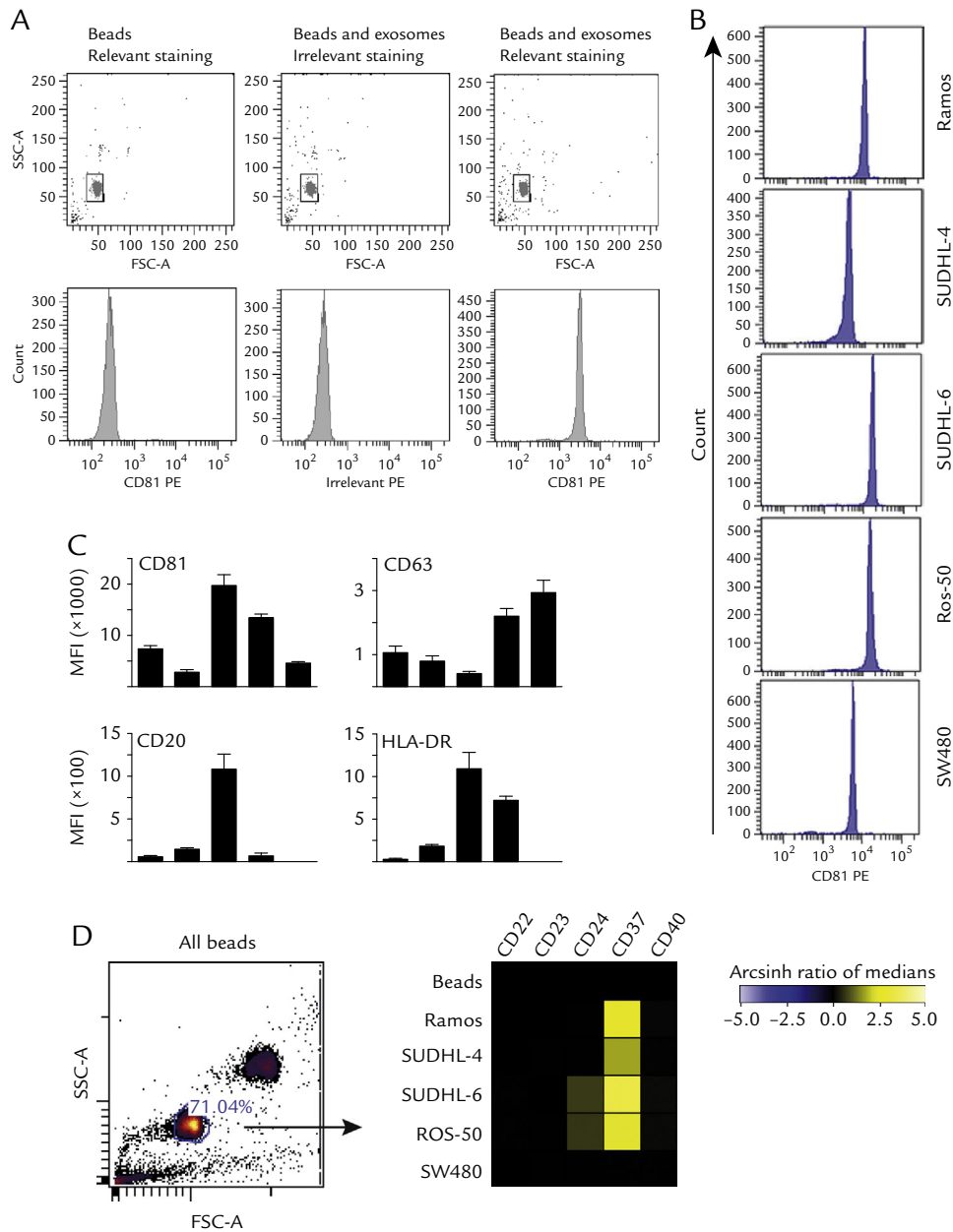


Figure 5. Expression of B-cell surface proteins and exosomal markers on exosomes. (A–D) CD63<sup>+</sup> (A, quantification in B) and CD81<sup>+</sup> (C, quantification in D) exosomes were immunisolated using anti-CD63 and anti-CD81 magnetic beads, respectively. Exosomes were lysed and processed for Western immunoblotting analysis. Expression of the B-cell surface proteins (CD19, HLA-DR, CD45, and CD20) and exosome markers (CD9, CD81, and CD63) were analyzed. IgG heavy chain was applied as the loading control. One of 3 representative Western immunoblots is shown. Quantification of B-cell surface antigens after isolation with anti-CD63 beads and anti-CD81 beads is presented in B and D, respectively. Mean (SEM) expression levels were measured as optical density (OD) and related to control using Image Lab software (n = 3). (E) Exosome isolated using anti-CD81 beads from media, ultracentrifugation (UC), and precipitation were analyzed. Samples were analyzed for the expression of CD81 and CD63 by Western immunoblotting.



**Figure 6.** Flow cytometric analysis of exosomes isolated with magnetic beads. Exosomes were immunisolated from preenriched exosome samples using magnetic beads coated with anti-human CD81. Exosomes were stained for B-cell surface antigens (CD20 HLA-DRD22, CD23, CD24, CD37, and CD40) and exosomal antigens (CD63 and CD81) followed by flow cytometric analysis and presented as median fluorescence intensity (MFI). (A) Scatterplot and fluorescence histogram of anti-CD81 beads in the absence of exosomes labeled for CD81 (left), anti-CD81 beads with exosomes stained with irrelevant fluorescent antibody (middle), and anti-CD81 beads with exosomes stained for CD81. (B) CD81<sup>+</sup> exosomes were isolated with magnetic beads coated with anti-human CD81 antibodies followed by staining of CD20 and HLA-DR in addition to the exosomal antigens CD81 and CD63. One of 3 representative experiments is shown. (C) Mean (SEM) quantification of the expression of CD81, CD63, CD20, and HLA-DR is shown (n = 3). (D) Expression of the B-cell surface proteins CD22, CD23, CD24, CD37, and CD40 on CD81<sup>+</sup> exosomes from the indicated B-cell lymphoma cell lines and SW480. Gating for single beads and MFI (arsinh ratio of medians relative to irrelevant control) are shown. Beads were applied as negative control. One of 3 representative experiments is shown. FSC-A = forward-scattered light ; PE = phycoerythrin; SSC-A = side-scattered light.

staining equals autofluorescence of the magnetic beads (Figure 6A) compared with the specific signal obtained by relevant CD81 staining of bead isolated exosomes (Figure 6A). Furthermore, additional control experiments were performed (see the [Supplementary Figure](#) in the online version at <http://dx.doi.org/10.1016/j.clinthera.2014.05.010>). Exosomes derived from the 4 different B-cell lymphoma cell lines in addition to SW480-derived exosomes were isolated with CD81 beads. After bead isolation, the exosomes were stained with anti-CD81 PE in the presence or absence of a blocking agent (normal mouse IgG). No significant difference in CD81 staining was observed in the presence or absence of a blocking reagent as indicated by flow cytometry (see the [Supplementary Figure](#) in the online version at <http://dx.doi.org/10.1016/j.clinthera.2014.05.010>). In addition, exosomes derived from 4 different B-cell lymphoma cell lines in addition to SW480-derived exosomes were isolated to target CD81 and stained with anti-CD81 PE (subclass IgG1) or anti-HLA-DR FITC (subclass IgG2b) in the presence or absence of blocking reagent (normal mouse IgG). No significant difference in CD81 or HLA-DR signal were observed (see the [Supplementary Figure](#) in the online version at <http://dx.doi.org/10.1016/j.clinthera.2014.05.010>).

CD81<sup>+</sup> exosomes were surface stained with antibodies against the B-cell surface proteins CD20 and HLA-DR, in addition to the exosome markers CD81 and CD63. The expression pattern of B-cell surface proteins and exosome markers revealed by Western immunoblotting analysis (Figure 5) was confirmed by FACS (Figures 6B and 6C). Figure 6B shows the flow cytometric analysis of a typical CD81 PE staining. The quantification of staining for CD81, CD63, CD20, and HLA-DR on isolated CD81<sup>+</sup> exosomes is presented in Figure 6C. For the CD81<sup>+</sup> isolated exosomes, samples from SUDHL-6 and Ros-50 had the most pronounced expression of CD81, whereas expression of CD63 was highest on exosomes from Ros-50 and SW480 cells (Figure 6C) confirmed by Western blotting (Figure 5C). Five other B-cell surface antigens (CD22, CD23, CD24, CD37, and CD40) were analyzed for expression on CD81<sup>+</sup> exosomes by flow cytometry. CD24 was expressed in exosomes derived from SUDHL-6 and Ros-50, whereas CD37 was highly expressed on exosomes from all cell lines, representing 4 different types of B-cell lymphoma (Figure 6D). These results are similar to the expression observed in the host cells (Figure 1B). However, among the other B-cell surface proteins,

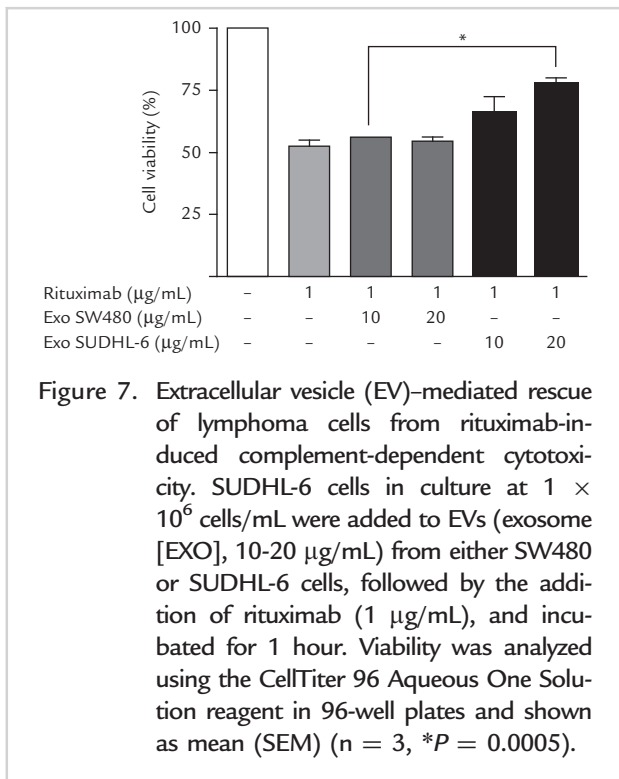
there are examples of high cellular expression and low or negative exosome expression (eg, CD22 and CD40). These findings illustrate that B-cell lymphoma-derived exosomes encompass variable expression of both B-cell surface proteins and classic exosomal markers. CD81 seemed to be the most widely expressed exosomal protein on exosomes released from B-cell lymphoma cells. CD81<sup>+</sup> exosomes were found to express CD19, CD20, HLA-DR, CD24, and CD37. All these B-cell surface proteins represent interesting targets for immunotherapy of B-cell lymphoma and other hematologic malignant neoplasms.

### EVs from Lymphoma Cells Intercept rituximab-induced CDC

Ligation of rituximab to CD20 exerts cytotoxic effects by induction of both CDC and antibody-dependent cell-mediated cytotoxicity. It has recently been found that ultracentrifuged exosomes from lymphoma cells can reduce rituximab-induced CDC in lymphoma cells. To know whether precipitated EVs had a similar interception of antibody-induced CDC, we applied a rituximab-mediated CDC assay to measure effects of adding EVs to lymphoma cells. SUDHL-6 cells treated with rituximab (1 µg/mL) alone had a 47% reduction in viability compared with untreated cells (Figure 7). When cells were preincubated with EVs (10-20 µg/mL) from CD20<sup>-</sup> SW480 cells before incubation with rituximab, no increase in viability was detected. In contrast, a significant improved viability (22% reduction) was measured when CD20<sup>+</sup> EVs from SUDHL-6 cells were added to the culture.

### DISCUSSION

A mean of 1 mL of blood serum, derived from healthy donors, contains approximately 10<sup>12</sup> exosomes. Depending on the disease, the number of exosomes can fluctuate. Concentration of exosomes in the bloodstream and all other body fluids is extremely high.<sup>52</sup> The aim of this study was to examine exosomes released from different B-cell lymphoma cell lines in terms of expression of B-cell surface antigens. We found that the level of typical exosomal markers and common B-cell markers diverge significantly, depending on the host cell origin. We have compared pre-enriched EVs with the more pure exosome fraction expressing CD81 and CD63 and also analyzed different subpopulations of exosomes. Our data clearly indicate a significant difference in protein composition



between precipitated EVs and bead isolated exosomes and importantly the existence of subpopulations of exosomes derived from the same cell type expressing their own characteristic panel of proteins. Exosomes derived from lymphoma B cells contain CD19, CD20, CD24, CD37, and HLA-DR, with a large heterogeneity among the different cell lines. These proteins represent interesting targets for immunotherapy, and in our work we found that CD20<sup>+</sup> EVs can intercept anti-CD20 (rituximab)-mediated cytotoxicity in lymphoma B cells.

In a recent review of EVs in cancer therapy,<sup>53</sup> one of the outstanding questions that was raised was whether subpopulations of EVs serve different physiologic functions. We believe that the immunomagnetic separation may represent one of the tools to study subpopulations of exosomes and to solve this important question. Enrichment of vesicles as small as exosomes is a challenging task. Such workflows often involve the use of ultracentrifugation with a sequential increase in centrifugal forces so that cellular components can stepwise be removed from the sample. In the final steps of such an elaborate protocol, exosomes are pulled out after centrifugation at 100,000g for >2 hours.<sup>14,22</sup> Exosomes obtained with ultracentrifugation appear heterogeneous in terms of size distribution, including 40- to 100-nm diameter vesicles,

but larger vesicles are also present.<sup>51</sup> In addition to contamination of larger vesicles, larger protein aggregates might coaggregate with the target vesicles. By floating the exosomes on a density gradient exploiting the exosomes' buoyant density during ultracentrifugation, protein aggregates can be removed from the exosome preparation. Exosomes enriched using density gradient centrifugation have a more homogenous appearance in terms of size distribution.<sup>51</sup> The protein profile revealed fewer proteins compared with exosomes prepared by ultracentrifugation, indicating that exosomes prepared by ultracentrifugation may be contaminated. As an alternative to an ultracentrifugation-based exosome enrichment, a precipitation-based exosome enrichment method might be used equivalent to precipitation of viruses and other smaller particles.<sup>53,54</sup> To increase the purity, Tauro et al<sup>51</sup> concluded that immunomagnetic separation was the best method for exosome capture. However, the immunomagnetic beads they used are in the nanometer range, a challenge in terms of resolution if the downstream application is flow cytometry, and it also requires an ultracentrifugation step to enrich the exosomes. This can be solved by providing a larger solid surface for the exosomes to dock, which can easily be observed in the flow cytometer. Clayton et al<sup>19</sup> developed a rapid and versatile technique for exosome isolation and flow analysis. Anti-major histocompatibility complex class II antibodies were coated to the surface of 4.5-μm magnetic beads. This bead size gives us a recognizable forward and side scatter pattern that allows for gating of single magnetic beads coated with exosomes for labeling analysis. The expression of B-cell surface proteins was limited in immunisolated CD81<sup>+</sup> and CD63<sup>+</sup> exosomes compared with microvesicles, indicating that by immunisolating CD81<sup>+</sup> and CD63<sup>+</sup> vesicles you will lose additional EVs that express B-cell surface proteins. These EVs can have the same potential in terms of immunotherapy interference compared with CD81<sup>+</sup> and CD63<sup>+</sup> exosomes. Yoshioka et al<sup>50</sup> have recently suggested CD9 and CD81 to be the most suitable exosome markers. However, CD9 is not expressed in all cell types (eg, mature B cells as reported here). We characterized exosomes derived from different B-cell lymphoma cell lines. This study provides evidence of release of CD81<sup>+</sup> exosomes expressing CD19, CD20, CD24, CD37, and HLA-DR from B-cell lymphoma cells. The exosomal expression of CD19 and CD20 was weak compared with the total EV pool, and CD45 was not detected in exosomes but well expressed in EVs. Our study of immunisolated

exosomes indicates a heterogeneous level of exosome release and expression of exosomal B-cell surface proteins among different B-cell lymphoma cell lines, representing different B-cell lymphoma subtypes.

Previous experiments have suggested a possible use of exosomes in cancer immunotherapy.<sup>1,55</sup> However, it has also been suggested that instead of augmenting immune responses exosomes mainly suppress anti-tumor immune responses.<sup>31,56</sup> Exosomes may therefore have positive and negative effects in terms of cancer progression. A deeper characterization of exosomes and their protein composition therefore justifies further studies of these vesicles to understand their relevance for tumor growth and metastasis and the molecular mechanisms mediating release of tumor cell-derived exosome and uptake in recipient cells.

In hematologic malignant neoplasms for which antibody-based cancer therapy is especially promising, it will be an advantage to characterize the expression of B-cell surface antigens on circulating exosomes. Exosomal CD19, CD20, CD37, and HLA-DR might intercept immunotherapy. We describe this for CD20, and a similar scenario may also be possible for antibodies against CD19, CD37, and HLA-DR, which currently are in clinical trials.<sup>33,39,57</sup> Although our work is supported by earlier findings of Aung et al,<sup>31</sup> who reported that B-cell surface markers are expressed on EVs released from B-cell lymphoma cell lines, there are also some discrepancies. Whereas we detect exosomal CD20 only in the SUDHL-6 cell line and not in the Ramos, SUDHL-4, or Ros-50 cell lines, Aung et al detected CD20<sup>+</sup> exosomes from SUDHL-4 cells. However, we were able to detect CD20<sup>+</sup> vesicles from SUDHL-4 and SUDHL-6 cells in our total EV precipitate (Figure 3). A significant difference in these 2 studies is the sample preparation of the EVs. Whereas Aung et al<sup>31</sup> used ultracentrifugation, we immunisolated CD81<sup>+</sup> and CD63<sup>+</sup> exosomes. The vesicles we are studying therefore represent a cleaner population of exosomes. Aung et al<sup>31</sup> also detected CD9 in exosomes released from SUDHL-4. This is surprising because CD9 should be expressed on pre-B cells and not on mature B-cells.<sup>58</sup>

## CONCLUSION

We found a large heterogeneity among the different B-cell lymphoma cell lines in terms of release of exosomes and their expression of B-cell surface antigens. B-cell surface antigens were detected on vesicles from a total EV precipitate and on immunisolated

CD81<sup>+</sup> and CD63<sup>+</sup> exosomes. CD81<sup>+</sup> exosomes expressed CD19, CD20, CD24, CD37, and HLA-DR, whereas HLA-DR was detected on CD63<sup>+</sup> exosomes. CD22, CD23, CD40, and CD45 were not detected on exosomes, although most of them are widely expressed in the B-cell lymphoma host cells. Similar to CD20, expression of B-cell surface antigens may intercept immunotherapy directed against these antigens, and it is therefore important to be aware of this and to further characterize exosomes released from B cells.

## ACKNOWLEDGMENTS

This work was supported by grant 41409 from the Research Council of Norway and grant 33260 from the Norwegian Cancer Society.

The authors would like to thank Lisbeth Larsen (Life Technologies), Marianne Smestad (Department of Biochemistry, Institute for Cancer Research), and Vera Hilden (Department of Immunology, Institute for Cancer Research) for technical assistance, Steinar Funderud and Jostein Dahle (Nordic Nanovector AS) for help with the anti-human CD37 antibody, and June H. Myklebust for discussions.

M.P. Oksvold was responsible for the experimental design, western blotting, data interpretation and writing of the manuscript. A. Kullman was responsible for the western blotting and flow cytometry analysis. L. Forfang was responsible for the flow cytometry analysis (on second flow instrument to confirm data. B. Kierulf was responsible for the flow assay development, flow assay validation and flow cyt analysis (on first flow instrument). M. Li was responsible for the miRNA analysis. A. Brech was responsible for the electron microscopy. A.V. Vlassov was responsible for the experimental design and miRNA analysis. E.B. Smeland was responsible for the writing of the manuscript. A. Neurauter was responsible for the experimental design, writing of the manuscript, and data interpretation. K.W. Pedersen was the project lead, and responsible for the experimental design, western blot method development, electron microscopy, writing of the manuscript, and data interpretation.

## CONFLICTS OF INTEREST

Anette Kullmann, Bente Kierulf, Axl Neurauter, Mu Li, Alexander V. Vlassov, and Ketil W. Pedersen are full-time employees of Life Technologies, Oslo, Norway. The authors have indicated that they have no other conflicts of interest regarding the content of this article.

## SUPPLEMENTAL MATERIAL

Supplemental figures accompanying this article can be found in the online version at <http://dx.doi.org/10.1016/j.clinthera.2014.05.010>.

## REFERENCES

- Bobrie A, Colombo M, Raposo G, Théry C. Exosome secretion: molecular mechanisms and roles in immune responses. *Traffic*. 2011;12:1659–1668.
- Théry C, Zitvogel L, Amigorena S. Exosomes: composition, biogenesis and function. *Nat Rev Immunol*. 2002;2:569–579.
- Janowska-Wieczorek M, Wysoczynski J, Kijowski L, Marquez-Curtis B, Machalinski J, Ratajczak MZ. Microvesicles derived from activated platelets induce metastasis and angiogenesis in lung cancer. *Int J Cancer*. 2005;113:752–760.
- Valadi H, Ekstrom K, Bossios A, Sjostrand M, Lee JJ, Lotvall JO. Exosome mediated transfer of mRNAs and microRNAs is a novel mechanism of genetic exchange between cells. *Nat Cell Biol*. 2007;9:654–659.
- Pegtel DM, van de Garde MD, Middeldorp JM. Viral miRNAs exploiting the endosomal-exosomal pathway for intercellular cross-talk and immune evasion. *Biochim Biophys Acta*. 2011;1809:715–721.
- Belting M, Wittrup A. Nanotubes, exosomes, and nucleic acid-binding peptides provide novel mechanisms of intercellular communication in eukaryotic cells: implications in health and disease. *J Cell Biol*. 2008;183:1187–1191.
- Mittelbrunn M, Gutiérrez-Vázquez C, Villarroya-Beltri C, et al. Unidirectional transfer of microRNA-loaded exosomes from T cells to antigen-presenting cells. *Nat Commun*. 2011;2:282.
- Skog J, Würdinger T, van Rijn S, et al. Glioblastoma microvesicles transport RNA and proteins that promote tumour growth and provide diagnostic biomarkers. *Nat Cell Biol*. 2008;10:1470–1476.
- Zomer A, Vendrig T, Hopmans ES, van Eijndhoven M, Middeldorp JM, Pegtel DM. Exosomes: fit to deliver small RNA. *Commun Integr Biol*. 2010;3:447–450.
- Lässer C, Eldh M, Lotvall J. Isolation and characterization of RNA-containing exosomes. *J Vis Exp*. 2012;59:3037.
- Mathivanan S, Simpson RJ. ExoCarta: a compendium of exosomal proteins and RNA. *Proteomics*. 2009;9:4997–5000.
- Conde-Vancells J, Rodriguez-Suarez E, Embade N, et al. Characterization and comprehensive proteome profiling of exosomes secreted by hepatocytes. *J Proteome Res*. 2008;7:5157–5166.
- Subra C, Grand D, Laulagnier K, et al. Exosomes account for vesicle-mediated transcellular transport of activatable phospholipases and prostaglandins. *J Lipid Res*. 2010;51:2105–2120.
- Théry C, Amigorena S, Raposo G, Clayton A. Isolation and characterization of exosomes from cell culture supernatants and biological fluids. *Curr Protocols Cell Biol*. 2006;3:22–30.
- Cheruvanky A, Zhou H, Pisitkun T, et al. Rapid isolation of urinary exosomal biomarkers using a nanomembrane ultrafiltration concentrator. *Am J Physiol Renal Physiol*. 2007;292:1657–1661.
- Munoz JL, Bliss SA, Greco SJ, Ramkissoon SH, Ligon KL, Rameshwar P. Delivery of functional anti-miR-9 by mesenchymal stem cell-derived exosomes to glioblastoma multiforme cells conferred chemosensitivity. *Mol Ther Nucleic Acids*. 2013;2:1–11.
- Zeng L, Wang G, Ummarino D, et al. Histone deacetylase 3 unconventional splicing mediates endothelial-to-mesenchymal transition through transforming growth factor  $\beta$ 2. *J Biol Chem*. 2013;288:31853–31866.
- Li Q, Eades G, Yao Y, Zhang Y, Xhou Q. Characterization of a stem-like subpopulation in basal-like ductal carcinoma in situ (DCIS) lesions. *J Biol Chem*. 2014;289:1303–1312.
- Clayton A, Court J, Navabi H, et al. Analysis of antigen presenting cell derived exosomes, based on immunomagnetic isolation and flow cytometry. *J Immunol Methods*. 2001;247:163–174.
- Chugh PE, Sin SH, Ozgur S, et al. Systemically circulating viral and tumor-derived microRNAs in KSHV-associated malignancies. *PLOS Pathog*. 2013;9:1–22.
- Al-Nedawi K, Meehan B, Micallef J, et al. Intercellular transfer of the oncogenic receptor EGFRvIII by microvesicles derived from tumour cells. *Nat Cell Biol*. 2008;10:619–624.
- Raposo G, Nijman HW, Stoorvogel W, et al. B lymphocytes secrete antigen-presenting vesicles. *J Exp Med*. 1996;183:1161–1172.
- Rialland P, Lankar D, Raposo G, Bonnerot C, Hubert P. BCR-bound antigen is targeted to exosomes in human follicular lymphoma B-cells. *Biol Cell*. 2006;98:491–501.
- Saunderson SC, Schubert PC, Dunn AC, et al. Induction of exosome release in primary B cells stimulated via CD40 and the IL-4 receptor. *J Immunol*. 2008;180:8146–8152.
- Arita S, Baba E, Shibata Y, et al. B cell activation regulates exosomal HLA production. *Eur J Immunol*. 2008;38:1423–1434.
- Holme PA, Solum NO, Brosstad F, et al. Demonstration of platelet-derived microvesicles in blood from patients with activated coagulation and fibrinolysis using a filtration technique and western blotting. *Thromb Haemost*. 1994;72:666–671.
- Hess C, Sadallah S, Hefti A, Landmann R, Schifferli JA. Ectosomes released by human neutrophils are specialized functional units. *J Immunol*. 1999;163:4564–4573.
- Cocucci E, Racchetti G, Meldolesi J. Shedding microvesicles: artefacts no more. *Trends Cell Biol*. 2009;19:43–51.
- Gyorgy B, Szabó TG, Pásztoi M, et al. Membrane vesicles, current state-of-the-art: emerging role of extracellular vesicles. *Cell Mol Life Sci*. 2011;68:2667–2688.
- Hartman ZC, Wei J, Glass OK, et al. Increasing vaccine potency through exosome antigen targeting. *Vaccine*. 2011;29:9361–9367.
- Aung T, Chapuy B, Vogel D, et al. Exosomal evasion of humoral immunotherapy in aggressive B-cell lymphoma

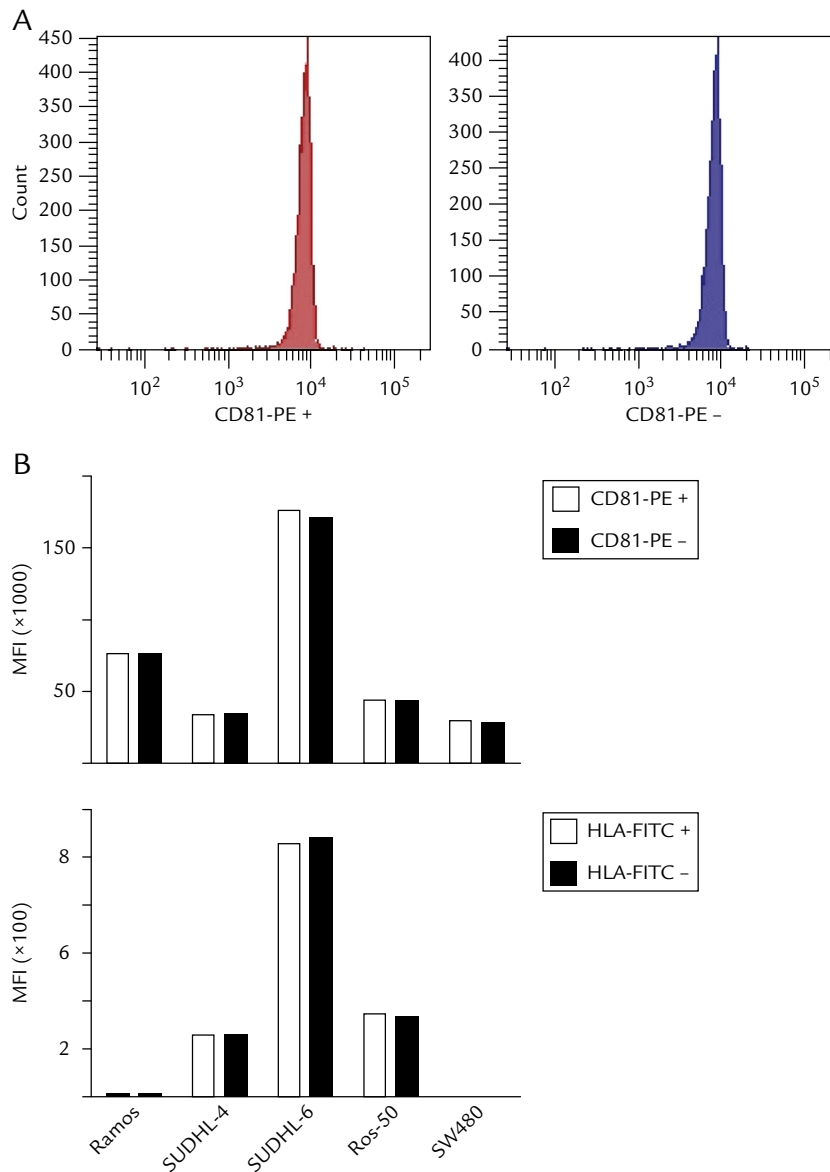
- modulated by ATP-binding cassette transporter A3. *Proc Natl Acad Sci U S A*. 2011;108:15336–15341.
32. Pagel JM, Pantelias A, Hedin N, et al. Evaluation of CD20, CD22, and HLA-DR targeting for radioimmunotherapy of B-cell lymphomas. *Cancer Res*. 2007;67:5921–5928.
  33. Blanc V, Bousseau A, Caron A, Carrez C, Lutz RJ, Lambert JM. SAR3419: an anti-CD19-maytansinoid immunoconjugate for the treatment of B-cell malignancies. *Clin Cancer Res*. 2011;17:6448–6458.
  34. Byrd JC, Kipps TJ, Flinn IW, et al. Phase 1/2 study of lumiliximab combined with fludarabine, cyclophosphamide, and rituximab in patients with relapsed or refractory chronic lymphocytic leukemia. *Blood*. 2010;115:489–495.
  35. Bodet-Milin C, Ferrer L, Pallardy A, et al. Radioimmunotherapy of B-cell non-Hodgkin's lymphoma. *Front Oncol*. 2013;3:1–13.
  36. Fonsatti E, Maio M, Altomonte M, Hersey P. Biology and clinical applications of CD40 in cancer treatment. *Semin Oncol*. 2010;37:517–523.
  37. DeNardo GL, Tobin E, Chan K, Bradt BM, DeNardo SJ. Direct anti-lymphoma effects on human lymphoma cells of monotherapy and combination therapy with CD20 and HLA-DR antibodies and 90Y-labeled HLA-DR antibodies. *Clin Cancer Res*. 2005;11:7075s–7079s.
  38. Pagel JM, Kenoyer AL, Bäck T, et al. Anti-CD45 pretargeted radioimmunotherapy using bismuth-213: high rates of complete remission and long-term survival in a mouse myeloid leukemia xenograft model. *Blood*. 2011;118:703–711.
  39. Tedder TF. CD19: a promising B cell target for rheumatoid arthritis. *Nat Rev Rheumatol*. 2009;5:572–577.
  40. Blomhoff HK, Smeland EB, Beiske K, et al. Cyclic AMP-mediated suppression of normal and neoplastic B cell proliferation is associated with regulation of myc and Ha-ras protooncogenes. *J Cell Physiol*. 1987;131:426–433.
  41. Zeringer E, Li M, Barta T, et al. Methods for the extraction and RNA profiling of exosomes. *World J Methodol*. 2013;3:11–18.
  42. Ericsson M, Cudmore S, Shuman S, Condit RC, Griffiths G, Krijnsse Locker J. Characterization of ts16, a temperature-sensitive mutant of vaccinia virus. *J Virol*. 1995;69:7072–7086.
  43. Bakkebo M, Huse K, Hilden VI, et al. SARA is dispensable for functional TGF- $\beta$  signaling. *FEBS Lett*. 2012;586:3367–3372.
  44. Mathivanan S, Ji H, Simpson RJ. Exosomes: extracellular organelles important in intercellular communication. *J Proteomics*. 2010;73:1907–1920.
  45. Pols MS, Klumperman J. Trafficking and function of the tetraspanin CD63. *Exp Cell Res*. 2009;315:1584–1592.
  46. Escola JM, Kleijmeer MJ, Stoorvogel W, Griffith JM, Yoshie O, Geuze HJ. Selective enrichment of tetraspan proteins on the internal vesicles of multivesicular endosomes and on exosomes secreted by human B-lymphocytes. *J Biol Chem*. 1998;273:20121–20127.
  47. Chiba M, Kimura M, Asari S. Exosomes secreted from human colorectal cancer cell lines contain mRNAs, microRNAs and natural antisense RNAs, that can transfer into the human hepatoma HepG2 and lung cancer A549 cell lines. *Ocol Rep*. 2012;28:1551–1558.
  48. Ginaldi L, De Martinis M, Matutes E, Farahat N, Morilla R, Catovsky D. Levels of expression of CD19 and CD20 in chronic B cell leukaemias. *J Clin Pathol*. 1998;51:364–369.
  49. Yu Y, Rabinowitz R, Polliack A, Ben-Bassat H, Schlesinger M. Hyposialated 185 kDa CD45RA<sup>+</sup> molecules attain a high concentration in B lymphoma cells and in activated human B cells. *Eur J Haematol*. 2002;68:22–30.
  50. Yoshioka Y, Konishi Y, Kosaka N, Katsuda T, Kato T, Ochiya T. Comparative marker analysis of extracellular vesicles in different human cancer types. *J Extracell Vesicles*. 2013;2:20424.
  51. Tauro BJ, Greening DW, Mathias RA, et al. Comparison of ultracentrifugation, density gradient separation, and immunoaffinity capture methods for isolating human colon cancer cell line LIM1863-derived exosomes. *Methods*. 2012;56:293–304.
  52. Schageman J, Zeringer E, Li M, et al. The complete exosome workflow solution: from isolation to characterization of RNA cargo. *Biomed Res Int*. 2013;2013:253957.
  53. Vader P, Breakfield XO, Wood MJA. Extracellular vesicles: emerging targets for cancer therapy. *Trends Mol Med*. 2 April 2014. [Epub ahead of print].
  54. Yamamoto KR, Alberts BM, Benzinger R, Lawhorne L, Treiber G. Rapid bacteriophage sedimentation in the presence of polyethylene glycol and its application to large-scale virus purification. *Virology*. 1970;40:734–744.
  55. Février B, Raposo G. Exosomes: endosomal-derived vesicles shipping extracellular messages. *Curr Opin Cell Biol*. 2004;16:415–421.
  56. Robbins PD, Morelli AE. Regulation of immune responses by extracellular vesicles. *Nat Rev Immunol*. 2014;14:195–208.
  57. Dahle J, Repetto-Llamazares AH, Mollatt CS, et al. Evaluating antigen targeting and anti-tumor activity of a new anti-CD37 radioimmunoconjugate against non-Hodgkin's lymphoma. *Anticancer Res*. 2013;33:85–95.
  58. Kersey JH, LeBien TW, Abramson CS, Newman R, Sutherland R, Greaves M. P-24: a human leukemia-associated and lymphohemopoietic progenitor cell surface structure identified with monoclonal antibody. *J Exp Med*. 1981;153:726–731.

---

**Address correspondence to:** Ketil W. Pedersen, Life Technologies AS, Ullernchausseen 52, PO Box 114 Smestad 0379 Oslo, Norway. E-mail: Ketil.pedersen@lifetech.com



## SUPPLEMENTARY MATERIALS



Supplementary Figure. The effect of blocking on staining efficiency. (A) Exosomes derived from SW480 cells were isolated with CD81 beads. After bead isolation, the exosomes were stained with CD81 phycoerythrin (PE) in the presence (left histogram) or absence (right histogram) of blocking reagent (normal mouse IgG). No significant difference in CD81 staining was observed in the presence or absence of blocking reagent. (B) Exosomes derived from 4 different B-cell lymphoma cell lines in addition to SW480 cell lines were isolated with CD81 beads and stained with CD81 PE (subclass IgG1) or HLA-DR fluorescein isothiocyanate (subclass IgG2b) in the presence or absence of blocking reagent (normal mouse IgG).